



Rapid prediction and compensation method of cutting force-induced error for thin-walled workpiece

Guangyan Ge¹ · Zhengchun Du¹ · Jianguo Yang¹

Received: 9 July 2019 / Accepted: 30 January 2020 / Published online: 10 February 2020
© Springer-Verlag London Ltd., part of Springer Nature 2020

Abstract

Significant machining errors may occur in thin-walled parts during the milling process due to their low rigidity. Conventionally, deformation prediction is conducted via the finite element method (FEM) due to its convenience and accuracy. However, it is extensively time-consuming because of the huge computation amount, which is caused by repeated computation of the displacements of all the nodes at each cutting location and iteration process. To solve this problem, a rapid deformation computation method based on stiffness matrix reduction was proposed. Furthermore, an iterative cutting force-induced error prediction model was established considering the tool-workpiece dynamic interaction, which shortened each cutting force-induced error prediction time from tens of seconds by traditional FEM to dozens of milliseconds. Lastly, the proposed method was applied to the compensation of thin-walled aluminum alloy blocks. The compensation experiment results revealed that the proposed model reduced the machining error by more than 53.6% with high real-time performance. This method demonstrates immense potential for further applications in deformation prediction of thin-walled freeform surface parts.

Keywords Thin-walled parts · Cutting force-induced error · Stiffness matrix reduction · Error compensation

1 Introduction

Today, milling low-rigidity or flexible parts with a large span ratio of height to thickness is a common manufacturing process, especially in the aerospace and power industries. However, significant machining errors may occur in thin-walled parts during the milling process due to their low rigidity, which seriously affects the machining accuracy, even causing failure of the workpiece [1]. In the machining process of thin-walled parts, cutting force-induced error accounts for the majority of machining errors, in the range of 40–70%. Therefore, many researchers have paid increasing attention to more efficient and accurate error prediction methods for low-rigidity parts.

There are mainly three types of strategies to predict and reduce the cutting force-induced errors: the finite element method (FEM), the processing parameters optimization method, and

analytical method. FEM is widely adopted due to its convenience. Kang et al. [2] proposed a systematic simulation procedure for surface form errors prediction in peripheral milling of a low rigid thin-walled workpiece, which included the judgment of contacts between the cutter and workpiece, and tool-workpiece deflection. Wang et al. [3] proposed a method that uses FEM to predict the deformation error during the spiral milling of blades. They corrected the blade model by combining the predicted error data with precision design requirements and adopted an error compensation scheme to improve the machining precision. Ibaraki et al. [4] developed an FEM-based model to simulate the deformation of a thin-walled workpiece during the milling process, which adopted an iterative algorithm to calculate the cutting force and deformation. Simeng et al. [5] proposed a milling error prediction method based on FEM, which considered both the spring back deformation of the workpiece and the material removal; the maximum prediction error of their method was less than 15%. Wang and Si [6] proposed a cutter-workpiece engagement extraction method to predict surface form errors caused by the milling force during the 5-axis flank milling process. They used an iterative scheme that considered the coupling effect between the cutting forces and tool-workpiece deformations; the maximum relative error rate of their simulation model was 18.8%.

✉ Zhengchun Du
zcd@sjtu.edu.cn

¹ School of Mechanical Engineering, Shanghai Jiao Tong University, Shanghai 200240, China

Processing parameters optimization method has also been widely studied by researchers. Li and Zhu [7] proposed a method to integrate the cutter runout effect into envelope surface modeling and adopted tool path optimization to improve the 5-axis machining accuracy. Gao et al. [8] identified a proper cutting parameter combination in milling difficult-to-machine material thin-walled parts and a deformation control strategy by tool path planning. Through compensation, the deformation decreased by more than 52.88%. Ibaraki et al. [9] proposed a cutting process optimization algorithm to obtain an optimized milling sequence that made the workpiece deformation smaller than the given threshold value. Experimental results revealed that the optimized tool path could reduce the milling error by 82%. Based on the on-machine measurement, Huang et al. [10] designed an iteration toolpath compensation algorithm to decrease the machining errors and avoid unwanted interference of 5-axis flank milling by modifying the toolpath; the maximum milling error decreased from 0.275 to 0.0829 mm.

Regarding the analytical methods, Kang et al. [11] proposed two efficient iterative algorithms named flexible iterative algorithm (FIAL) and double iterative algorithm (DIAL) to predict surface form errors and calculate the positions and magnitude of the maximum surface form errors, respectively. The experimental results demonstrated that FIAL is faster in the iteration convergent speed and DIAL is valid in the maximum error prediction. Li and Zhu [12] developed a method to obtain cutter workpiece engagement (CWE) boundaries in 5-axis milling with a general tool that integrates the cutter runout impact and conducted cutting force comparison experiments to prove the higher prediction accuracy of their method. Tuysuz and Altintas [13] developed a reduced-order workpiece dynamic parameter update model using substructuring and perturbation methods, which is approximately four times more computationally efficient than the frequency-domain model.

From previous literatures, it can be inferred that reducing cutting force induced errors offline is a more economical method, while using the analytical model is more efficient and accurate. However, most milling force analytical models are complicated, and deformations of thin-walled workpieces caused by the cutting force in most cases are computed by the traditional FEM along with the GUI method, which feature relatively low prediction efficiency. Therefore, calculation and prediction of the cutting force inducing error or deformation in an efficient and accurate manner is a challenging task, especially when considering the tool-workpiece dynamic interaction, which results in a heavy burden to the traditional FE computation. Focusing on the efficiency problem, this study proposes a rapid cutting force-induced error prediction method for thin-walled parts considering the tool-workpiece dynamic interaction based on the global stiffness matrix.

The rest of this paper is organized as follows: in Section 2, a rapid deformation computation method based on stiffness

matrix reduction is proposed, which establishes the foundation of a novel error prediction model that considers the tool-workpiece dynamic interaction. An iterative cutting force-induced error prediction method based on the rapid deformation computation method is proposed and compared with the traditional FE computation method in Section 3. The 4th section describes the application of the iterative cutting force-induced error prediction method through a compensation experiment. The last section states the final conclusions.

2 The rapid deformation computation method

Conventionally, deformations of the workpiece under a certain value of cutting force are usually obtained via FEM due to its convenience and accuracy. However, it is extensively time-consuming because of the huge computation amount, which is caused by repeatedly solving a large set of equations at each change of the applied force. Therefore, a rapid deformation computation method that can calculate the deformations of arbitrary points within a few milliseconds is proposed in this section.

2.1 The deformation model of the workpiece

The workpiece is usually considered as an elastic body and discretized into finite elements when applying to the FEM static structure analysis. Assuming that the deformation of the workpiece is within the elastic limit range and satisfies Hooke's law. The nodes in the FEM model can be divided into two types: the nodes on the machining surface, which is represented as preserve nodes {P}, and the nodes that are not on the machining surface, which is represented as reduced nodes {R}. In order to efficiently compute the deformation of each cutting location, the deformation of {P} is mainly focus in the milling process, so the deformation solving process can be reduced to the deformation solving of the machining surface, as shown in Fig. 1. The detailed reduction process is as follows.

The static equilibrium equation of the workpiece under acting force F is usually expressed as:

$$K \cdot x = F \quad (1)$$

where K is the global stiffness matrix of the workpiece and x is the displacement of all the nodes. According to the node type, Eq. (1) can be expanded as:

$$\begin{bmatrix} K_{pp} & K_{pr} \\ K_{rp} & K_{rr} \end{bmatrix} \begin{bmatrix} x_p \\ x_r \end{bmatrix} = \begin{bmatrix} F_p \\ F_r \end{bmatrix} \quad (2)$$

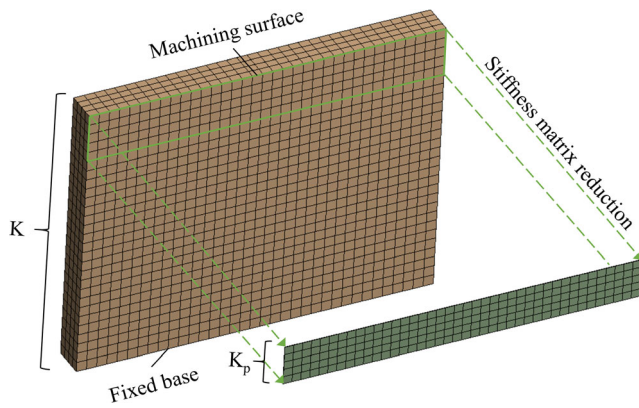


Fig. 1 Reduction of global stiffness matrix

where K_{pp} , K_{pr} , K_{rp} , K_{rr} , are the matrices partitioned according to the node type, x_p is the displacements of the preserve nodes {P}, x_r is the displacements of the reduced nodes {R}, F_p , and F_r are the cutting forces on {P} and {R}, respectively.

The deformation of the cutter-workpiece engagement area is mainly focused on the cutting force-induced deformation analysis. In the machining process, the cutting force is always acting on the machining surface, so F_r is to be zero. Substituting F_r to Eq. (2), the displacements of {R} is expressed as:

$$x_r = -K_{rr}^{-1}K_{rp}x_p \tag{3}$$

Thus, the milling force, which is also the acting force on {P} can be expressed as:

$$F_p = (K_{pp} - K_{pr}K_{rr}^{-1}K_{rp})x_p = K_p x_p \tag{4}$$

Furthermore, the reduced stiffness matrix K_p is obtained as:

$$K_p = T_s^T K T_s \tag{5}$$

where

$$T_s = \begin{bmatrix} I \\ -K_{rr}^{-1}K_{rp} \end{bmatrix}$$

represents the static transformation matrix between global stiffness matrix K and reduced stiffness matrix K_p .

Through the above reduction process, the static displacements of the nodes on the milling surface are:

$$x_p = K_p^{-1} F_p \tag{6}$$

Compared with Eq.(1), the degrees of freedom that require solving in Eq. (6) are reduced from the dimension of K to the

dimension of K_p . As the dimension of K far outweighs that of K_p , the computational efficiency can be significantly improved. Moreover, the structural complexity remains the same because all elements of the original global stiffness matrix contribute. Although the damping and inertia are ignored in the reduction, it will not affect the prediction accuracy of static structure analysis.

The three-dimension displacement of one node on the machining surface is:

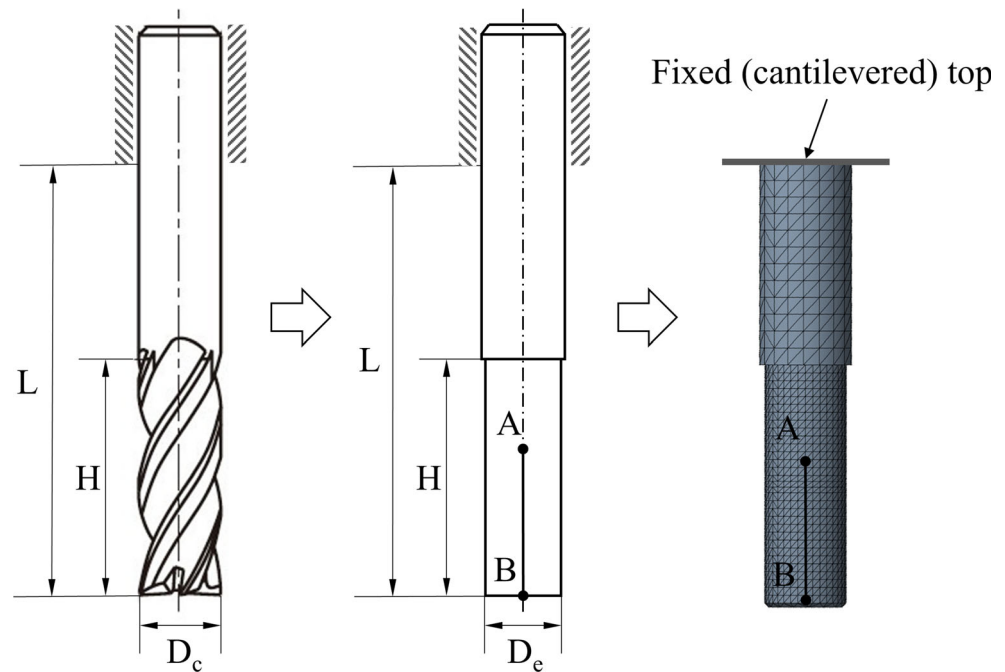
$$\begin{bmatrix} x_x \\ x_y \\ x_z \\ x_i \end{bmatrix} = \underbrace{\begin{bmatrix} s_{1xx} & s_{1xy} & s_{1xz} & \cdots & s_{nxx} & s_{nxy} & s_{nxz} \\ s_{1yx} & s_{1yy} & s_{1yz} & \cdots & s_{nyx} & s_{nyy} & s_{nyz} \\ s_{1zx} & s_{1zy} & s_{1zz} & \cdots & s_{nzx} & s_{nzy} & s_{nzz} \end{bmatrix}}_{S_i} \cdot \begin{bmatrix} (f_{1x} & f_{1y} & f_{1z})^T \\ \vdots & \vdots & \vdots \\ (f_{nx} & f_{ny} & f_{nz})^T \end{bmatrix}_{F_p} \tag{7}$$

where x_i is the three-dimension displacement of node i , S_i is the compliance of node i , s_{muv} is the v direction displacement of node i caused by u direction force component on point n , F_p is the force on all the nodes on the machining surface. Referring to Eq. (6), it can be deduced that x_i in Eq. (7) is actually the $(3i-2)_{th}$, $(3i-1)_{th}$, and $(3i)_{th}$ row of x in Eq. (6). In addition, S_i corresponds to the $(3i-2)_{th}$, $(3i-1)_{th}$, and $(3i)_{th}$ row of K_p^{-1} . Thus, the displacements of each cutting location can be obtained through Eq. (7), which requires only $3n$ multiplications and additions. Due to the change of milling force at each cutting location, the FEM needs to repetitively compute the deformation of the workpiece using Eq. (1), which requires the inverse of an $n \times n$ stiffness matrix. Normally, the inverse operation of an $n \times n$ matrix has a computational complexity of $O(n^3)$. Therefore, it is considered that this method reduces the computation complexity from $O(n^3)$ to $O(3n)$.

2.2 The deformation model of the cutter

The milling tool is modeled as a cantilevered elastic beam with the tool diameter equivalent to $D_e = s \cdot D_s$ ($s \approx 0.8$), where D_s was the diameter of the shank and s was the scaling factor accounting for the helical flutes, as shown in Fig. 2. The scaling factor s is calculated based on the model of Kops and Vo [14] according to the principle of equivalent rigidity, which considered the influence of flute number and helix angle. This simplification model is widely used in related works [15] for its efficiency and accuracy. The cutting force is considered to be distributed uniformly along the cutting depth line AB. As the rotational speed of the tool far outweighs the federate and the contact length of the cutter and workpiece is relatively short, the contact state between the cutter and workpiece can be considered as an equivalent invariant line AB.

Fig. 2 Equivalent model of the cutter



The deformation of the cutter is also computed through the above stiffness matrix reduction method. The deformation of point B is calculated as the cutting point deformation of the cutter. Because the cutting force is simplified as a linear distributed force, which acts on the nodes of line AB, the global stiffness matrix of the cutter can be reduced to the stiffness matrix of dozens of nodes. Thus, the deformation computation amount of the cutter is significantly small.

The above proposed rapid deformation computation method is able to obtain the deformation of the workpiece and the cutter at arbitrary cutting location with high efficiency, which establishes a foundation for the following iteration algorithm and real-time cutting force-induced error compensation.

3 The iterative cutting force-induced error prediction method

The deformation of the cutter and the workpiece can be separately calculated using the above rapid deformation computation method. However, the cutting-force-induced error is not the simple addition of tool deformation and workpiece deformation due to the coupling effect between them. Thus, we propose an iterative cutting-force-induced error prediction method in this section.

3.1 The iterative cutting force-induced error prediction method

One important step of the iterative cutting force-induced error prediction method is solving and updating the cutting force.

Here, we adopted an infinitesimal cutting force model due to its high computation speed and good adaptability. According to the results in Ref. [16], the infinitesimal-element cutting process of the tool can be illustrated as shown in Fig. 3.

The cutting force can be regarded as a periodic function with a period of 2π . Through the coordinate transform and Fourier transform, the overall cutting force analysis formula can be expressed as:

$$F(n) = \frac{z}{2\pi} \int_0^{2\pi} e^{-jn\frac{h}{R}} [A_1 S_1(n) + A_2 S_2(n)] dh, \quad n = 0, Z, 2Z, 3Z \dots \quad (8)$$

where

$$A_1 = \begin{bmatrix} -k_{ts} & -k_{rs} & 0 \\ k_{rs} & k_{ts} & 0 \\ 0 & 0 & -k_{as} \end{bmatrix}, \quad A_2 = \begin{bmatrix} -k_{ps} & -k_{rp} & 0 \\ k_{rp} & k_{tp} & 0 \\ 0 & 0 & -k_{ap} \end{bmatrix}$$

$$B_1(\theta) = \begin{bmatrix} \sin\theta \cos\theta \\ \sin^2\theta \\ \sin\theta \end{bmatrix}, \quad B_2(\theta) = \begin{bmatrix} \cos\theta \\ \sin\theta \\ 1 \end{bmatrix}$$

k_{ts} , k_{rs} , and k_{as} are the shear force tangential, radial, and axial milling coefficients, respectively; k_{tp} , k_{rp} , and k_{ap} are the plow tangential, radial, and axial milling coefficients, respectively. The above coefficients vary with different materials and different cutters, so the calibration is needed before practical application.

The dynamic interaction between the cutter and workpiece can be concretely described as: the deformation of the cutter and workpiece reduces the radial cutting depth dr and the cutting force F , which conversely increases the deformation

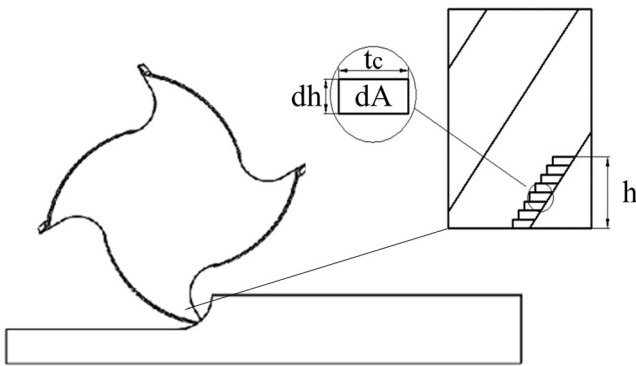


Fig. 3 Infinitesimal-element cutting process

cutting depth and the cutting force. This negative feedback process constantly repeats until it achieves a given convergence threshold.

The flowchart of the iterative cutting force-induced error prediction algorithm is shown in Fig. 4. First, the stiffness matrices of the cutter and workpiece are reduced using the repaid deformation computation method proposed in Section 2. Second, the iterative cutting force and the resultant displacement of the cutter and workpiece are computed until the convergence threshold is reached. The above process repeats at each cutting location to compute the cutting force-induced errors of the whole cutting process.

Although with the iteration considered, the computation amount of the cutting force-induced error has still been reduced to a significant level by the above proposed rapid computation method, which is efficient enough to complete one iterative computation within a few milliseconds. Because the establishment and reduction of stiffness matrix take much more time, in order to satisfy the high real-time requirements of the compensation system, the establishment and reduction of the stiffness matrix of the cutter and workpiece are completed in the preprocess, while the iterative cutting force and displacements are computed during the milling process with the real-time input of the coordinate of cutting location.

3.2 Verification of accuracy and efficiency

To verify the accuracy and efficiency of the proposed iterative cutting force-induced error prediction method (ICEPM), the cutting force-induced errors of 12 cutting locations of a thin-walled workpiece, which are shown in Fig. 5, were computed using the above method. The workpiece was a base-fixed 6061-aluminum alloy block with dimensions of $90 \times 70 \times 8$ mm.

The cutter radius, axial cutting depth, radial cutting depth, and feed speed per tooth were set to 4.5 mm, 1 mm, 6 mm, and 0.05 mm/tooth, respectively. The parameters of the FE models of the workpiece and cutter are listed in Table 1. As shown in Fig. 6, the workpiece was meshed with three different mesh densities to reach both high computation accuracy on the

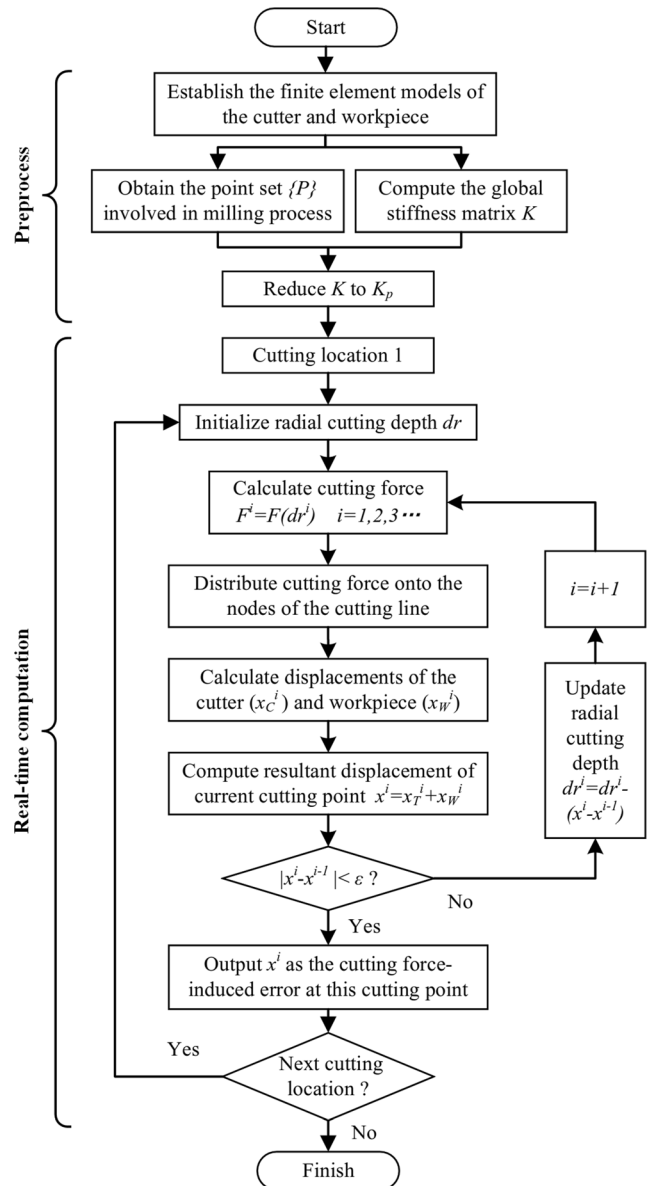


Fig. 4 Flowchart of the iterative cutting force-induced error prediction method

machining surface and the high computation efficiency on the rest areas. The convergence threshold was set to 0.1% relative error.

The computation was conducted on a computer with an Intel Xeon E5–2678 v3 processor and 64G DDR4 DRAM. It took 3.3 mins to complete the preprocess, which included the establishment and reduction of the FE models of the cutter and workpiece. The iterative computation for cutting force-induced error was then performed. The computation time for each cutting force-induced error was logged.

In the meantime, to compare the computation time, the same prediction was carried out using a similar iterative prediction method based on the traditional FEM software. The FE models of the workpiece and milling tool used were the same

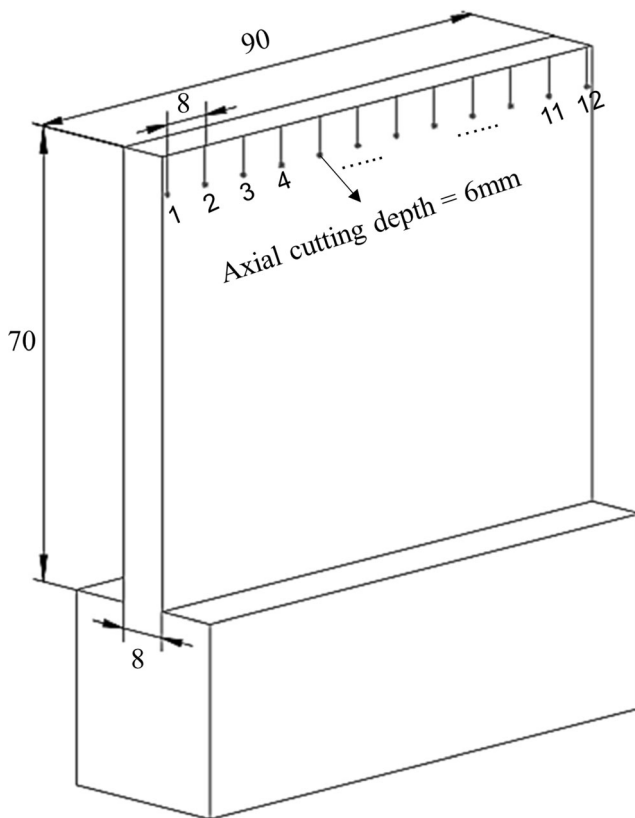


Fig. 5 Cutting locations

as in the ICEPM, as well as the cutting force model parameters and the given threshold. The core difference was that the displacements of the cutting locations were obtained completely through the FEM instead of through the rapid deformation computation method proposed in section 2.2. It took about 3.5 mins to complete the preprocess, which consisted of setting up the automatic modeling, meshing, loading, solving, and outputting deformation of different locations.

The iteration numbers of the above two methods were coincident, most of which were between 3 and 5. The comparisons of the predicted cutting force-induced error and computation time for each cutting location are shown in Fig. 7. The predicted error values of the ICEPM and FE iteration method are essentially in agreement with each other and the maximum relative error was 1.416%. However, the computation efficiency of ICEPM was thousands of times lesser than that of the FE iteration method, which has been shortened from tens of seconds to dozens of milliseconds. Thus, it can be concluded that the proposed method can reach the approximate accuracy as

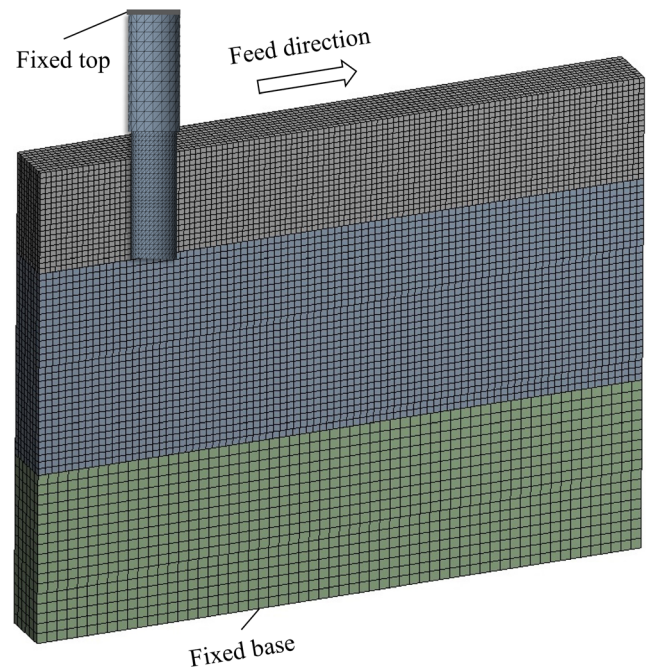


Fig. 6 Milling tool finite element model

that of the FE iteration method, in addition to being hundred times more efficient.

4 Application case

To demonstrate the engineering capacity to improve the machining precision of thin-walled parts, the iterative cutting force-induced error prediction method was applied to the compensation experiment of thin-walled aluminum alloy blocks.

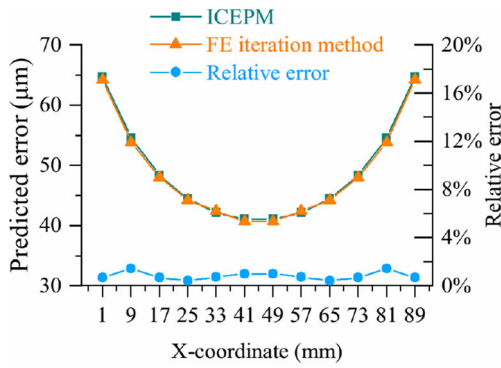
4.1 Development of the compensation system

As shown in Fig. 8, the cutting force-induced error compensation system was developed based on the external machine zero point shift (EMZPS) function of a Fanuc system, which was achieved by moving the tool or workpiece in the opposite direction between the tool and workpiece to create a new error to offset the original comprehensive errors.

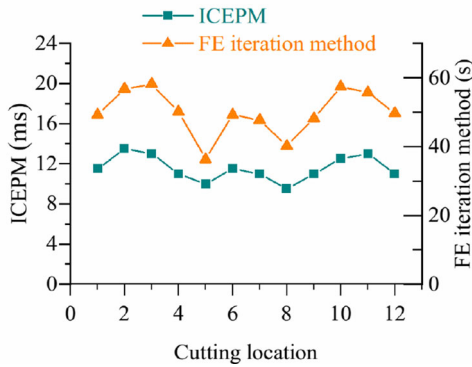
The principle diagrams of error compensation and its system structure are shown in Fig. 9. The error model is established by the proposed prediction model and the error values are computed on the main arithmetic unit. The real-

Table 1 FE models setup

Object	Density (kg/m ³)	Young's Modulus	Poisson ratio	Nodes number	Boundary condition
Workpiece	2800	68.9 GPa	0.33	223,296	Fixed base
Cutter	1480	210 Gpa	0.21	15,485	Fixed top



(a) Comparison of error prediction



(b) Comparison of computation time

Fig. 7 Comparison of ICEPM and FE iteration method

time position information of the machine is obtained through the network interface. The compensation values are transmitted to the numerical control system. Then the compensation values are added to the coordinate of X, Y, Z, axes to compensate the cutting force-induced error.

However, due to the periodic change of the coordinates, the compensation system may cause the cutting depth and cutting force to fluctuate, which further exciting relative vibration between the cutter and workpiece and leave chatter patterns

on the surface of workpiece. Thus, the stability of the compensation was analyzed.

The compensation period T of the developed system is adjustable from 40 ms to 200 ms. The compensation amplitude A is decided by the compensation period T , the feed speed V_f , current coordinate c and the cutting force-induced error value x :

$$A = \frac{x(V_f \cdot T + c) - x(c)}{T} \tag{9}$$

It can be calculated that the compensation amplitude is relatively small under common cutting parameters, for example, the compensation amplitudes of all the cutting locations are within 1 μm in the experiment of this section. Thus, the vibration of the cutting force caused by the compensation system can be ignored in this case.

4.2 Experiment setup

The peripheral milling experiment of thin-walled parts was conducted on a VMC850E vertical machining center. The tool was a carbide milling cutter, with four blades of 12 mm diameter, and a helix angle of 30°. The workpiece was a 6061-aluminum alloy block with the dimensions of 90 × 70 × 8 mm. The cutting force in the milling process was measured by a 9257B type 3D force dynamometer. The precision of the workpiece after machining was measured by a V3696 coordinate measuring machine, the accuracy of which was (2.5 + L/300) μm . The experimental temperature was 20 °C.

As shown in Figs. 10, eight sets of experiments were conducted on the same workpiece to reduce the repeated clamping error. The cutting force-induced error was predicted with the proposed iterative cutting force-induced error prediction model and then, was computed and compensated in real-

Fig. 8 Error compensation system

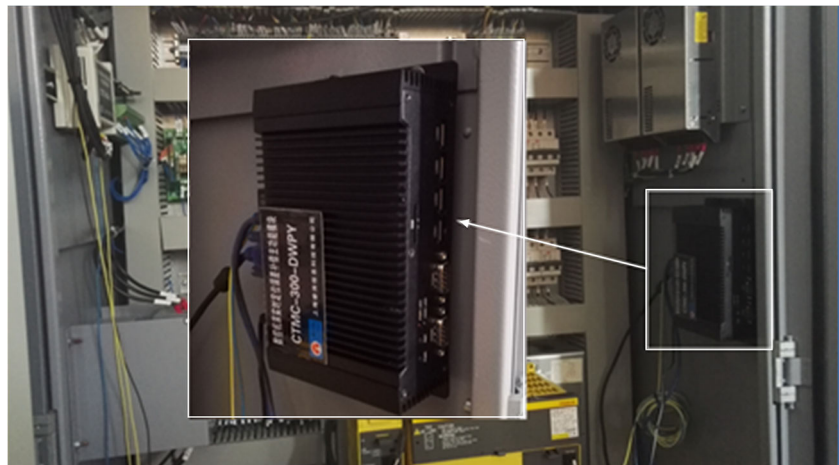
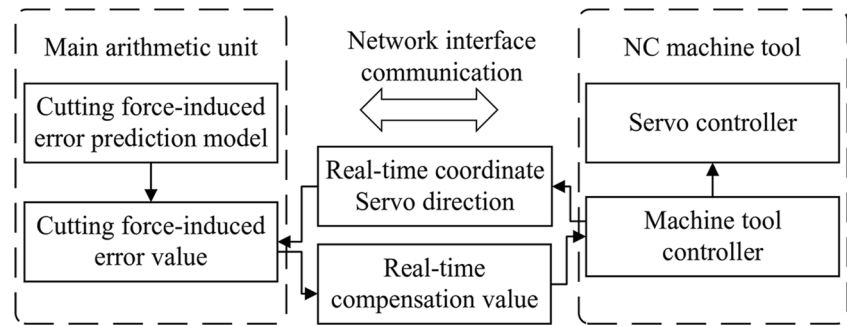


Fig. 9 The principle of error compensation system



time. Cutting processes without compensation and with cutting force-induced error compensation were conducted under the two parameters listed in Table 2, respectively.

In peripheral milling, the milling cutter has the largest influence on the deformation of the workpiece along the radial direction. Thus, only the deformation along the radial direction (the y -axis) was considered in this case. The processing procedure and the comparison between before and after processing are shown in Fig. 10. Blocks 1 and 2 were processed according to parameter 1 with cutting force-induced error compensation. Blocks 3 and 4 were processed according to parameter 1 without compensation. Blocks 5 and 6 were processed according to parameter 2 with cutting force-induced error compensation. Blocks 7 and 8 were processed according to parameter 2 without compensation.

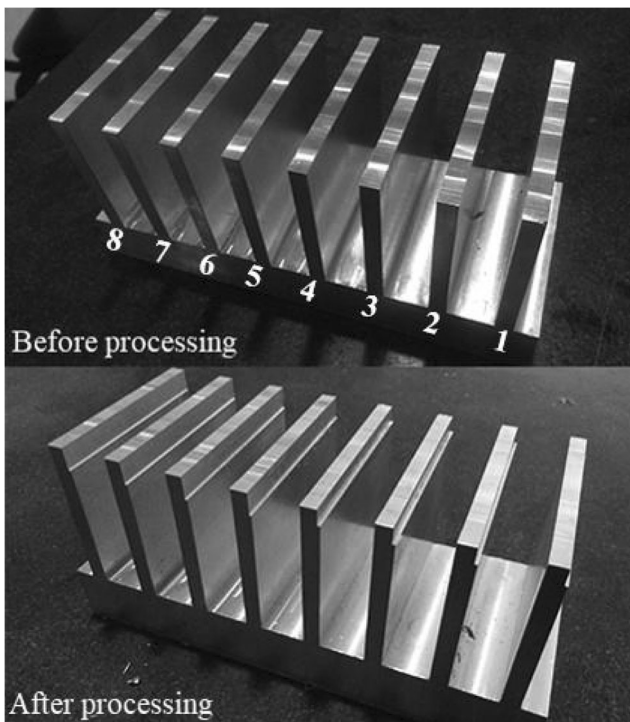


Fig. 10 Comparison between before and after processing

5 Results and discussion

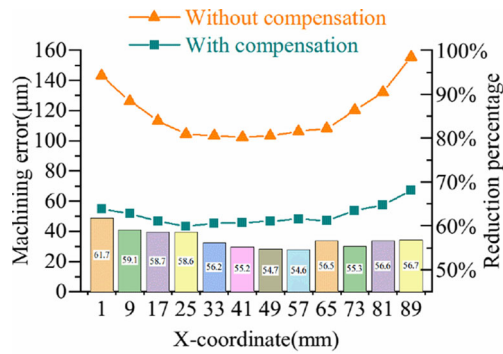
The machining errors of 12 equidistant points at the top of the workpiece were measured by a coordinate measuring machine. As shown in Fig. 11, for the machining parameter set 1, the initial average error was $118 \mu\text{m}$, and it was decreased to $50 \mu\text{m}$ after the cutting force-induced error compensation; the minimum reduction percentage of the machining error was 54.5%. For machining parameter 2, the average error was decreased from $159 \mu\text{m}$ to $71 \mu\text{m}$ after the cutting force-induced error compensation; the minimum reduction percentage of the machining error was 53.6%. Also, the proposed iterative method demonstrated high real-time performance during the compensation process.

The above experimental data reveals that the machining error has been reduced by more than 53.6%, which proves that the proposed iterative cutting force-induced error prediction method can significantly improve the machining precision of the milling of thin-walled parts. In addition, the pre-processing time was within 4 mins and the computation time of each cutting location was within 20 ms , which has showed high real-time performance and future possibility of industrial applications. However, due to the complexity of the machining error sources, other error sources, such as geometric errors or thermal errors, were not compensated in this experiment, which limited the machining accuracy improvement.

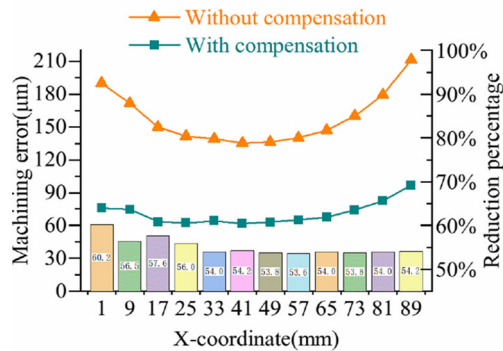
In fact, the proposed method can also be applied to the deformation computation of changing stiffness matrix but with lower efficiency, which is caused by repetitive reduction process. However, this study aims to propose an efficient method to improve the machining accuracy of the finish machining, in which the material removal rate is low and the

Table 2 Peripheral milling parameters

No.	Spindle speed (r/min)	Feed per tooth (mm/z)	Axial cutting depth (mm)	Radial cutting depth (mm)
1	1000	0.05	7	1.5
2	1000	0.05	10	1



(a) Accuracy of workpiece under machining parameters set 1



(b) Accuracy of workpiece under machining parameters set 2

Fig. 11 Comparison of absolute errors at the top of workpiece

change of the stiffness matrix is small. The computation cost and prediction accuracy of not considering and considering material removal for the Experiment set #1 in Section 4.2 were compared. The result shows that their accuracy difference is less than 3.6% but the latter cost hundreds times of computation time. Thus, in this study, the stiffness matrix change is ignored for the consideration of efficiency and without losing much accuracy.

6 Conclusions

Based on the above analyzes, the following conclusions are drawn:

- (1) This study established an iterative cutting force-induced error prediction method based on the stiffness matrix reduction of the cutter and workpiece, which considered the negative feedback dynamic interaction between the cutter and workpiece and performed cutting force-induced error prediction of each cutting location within dozens of milliseconds.
- (2) The iterative cutting force-induced error prediction method was applied to the compensation experiment of thin-walled aluminum alloy blocks, based on a real-time error compensation system developed by using the EMZPS function of a Fanuc numerical system. Through the

application case, the precision of two situations (without compensation and with cutting force-induced error compensation) in two processing parameters were compared. The results showed that the machining error was reduced by more than 53.6% with high real-time performance, which verified the validity. In addition, the pre-processing time of the proposed method was within 4 mins and the computation time of each cutting location was within 20 ms, which demonstrates future possibility of industrial applications.

- (3) The proposed iterative method shows effective engineering capacity to improve the machining precision and efficiency of thin-walled parts, as well as immense potential in the further application of thin-walled freeform surface parts. However, other error sources, such as geometric errors, or thermal errors were not compensated in this experiment, which limited the machining accuracy improvement. In addition, considering the computation efficiency, the material removal was not considered in this study. The proposed method will be further developed for the machining of 5-axis thin-walled parts. Furthermore, the material removal, dynamic change of cutting thickness, and other key influencing factors will be taken into consideration in our future researches.

Funding information The authors would like to express their thanks for the gracious financial support from National Key Research and Development Project of China (No. 2018YFB1701204) and National Natural Science Foundation of China (No. 51975372). Also, the authors would like to thank Manufacturing Research Center, Georgia Institute of Technology, for offering the opportunity to conduct the research of the analytical cutting force model and error compensation.

References

1. Ratchev S, Liu S, Huang W, Becker AA (2006) An advanced FEA based force induced error compensation strategy in milling. *Int J Mach Tools Manuf* 46:542–551
2. Kang YG, Yang GR, Huang J, Zhu JH (2014) Systematic simulation method for the calculation of maximum deflections in peripheral milling of thin-walled Workpieces with flexible iterative algorithms. *Adv Mater Res* 909:185–191
3. Wang MH, Sun Y (2014) Error prediction and compensation based on interference-free tool paths in blade milling. *Int J Adv Manuf Technol* 71:1309–1318
4. Wang J, Ibaraki S, Matsubara A, Shida K, Yamada T (2015) FEM-based simulation for workpiece deformation in thin-wall milling. *Int J Autom Technol* 9:122–128
5. Si-meng L, Xiao-dong S, Xiao-bo G, Dou W (2017) Simulation of the deformation caused by the machining cutting force on thin-walled deep cavity parts. *Int J Adv Manuf Technol* 92:3503–3517
6. Wang L, Si H (2018) Machining deformation prediction of thin-walled workpieces in five-axis flank milling. *Int J Adv Manuf Technol* 97:4179–4193
7. Li ZL, Zhu LM (2014) Envelope surface modeling and tool path optimization for five-Axis flank milling considering cutter Runout. *J Manuf Sci Eng* 136:041021

8. Gao Y, Ma J, Jia Z, Wang F, Si L, Song D (2016) Tool path planning and machining deformation compensation in high-speed milling for difficult-to-machine material thin-walled parts with curved surface. *Int J Adv Manuf Technol* 84:1757–1767
9. Wang J, Ibaraki S, Matsubara A (2017) A cutting sequence optimization algorithm to reduce the workpiece deformation in thin-wall machining. *Precis Eng* 50:506–514
10. Huang N, Bi Q, Wang Y, Sun C (2014) 5-Axis adaptive flank milling of flexible thin-walled parts based on the on-machine measurement. *Int J Mach Tools Manuf* 84:1–8
11. Kang YG, Wang ZQ (2013) Two efficient iterative algorithms for error prediction in peripheral milling of thin-walled workpieces considering the in-cutting chip. *Int J Mach Tools Manuf* 73:55–61
12. Li ZL, Zhu LM (2017) An accurate method for determining cutter-workpiece engagements in five-axis milling with a general tool considering cutter runout. *J Manuf Sci Eng Trans ASME* 140:021001
13. Tuysuz O, Altintas Y (2017) Time domain modeling of varying dynamic characteristics in Thin-Wall machining using perturbation and reduced order substructuring methods. *J Manuf Sci Eng Trans ASME* 140:011015
14. Kops L, Vo DT (1990) Determination of the equivalent diameter of an end mill based on its compliance. *CIRP Ann - Manuf Technol* 39:93–96
15. Wan M, Zhang W, Qiu K, Gao T, Yang Y (2005) Numerical prediction of static form errors in peripheral milling of thin-walled Workpieces with irregular meshes. *J Manuf Sci Eng* 127:13
16. Du Z, Zhang D, Hou H, Liang S (2017) Peripheral milling force induced error compensation using analytical force model and APDL deformation calculation. *Int J Adv Manuf Technol* 88:3405–3417

Publisher's note Springer Nature remains neutral with regard to jurisdictional claims in published maps and institutional affiliations.